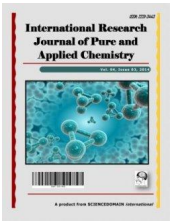

International Research Journal of Pure & Applied Chemistry
9(3): 1-6, 2015, Article no.IRJPAC.19579
ISSN: 2231-3443

SCIENCEDOMAIN *international*
www.sciencedomain.org

Theoretical Calculation of Antigen-Antibody Interactions for the Development of Antibody Based Filters

Mohidus Samad Khan[1,2*], Michael A. Whitehead[1] and Theo G. M. van de Ven[1*]

[1]Department of Chemistry, McGill University, 3420 University Street, Montreal, Quebec, H3A 2A7, Canada.
[2]Department of Chemical Engineering, Bangladesh University of Engineering and Technology, Dhaka 1000, Bangladesh.

Authors' contributions

This work was carried out in collaboration between all authors. All authors read and approved the final manuscript.

Article Information

DOI: 10.9734/IRJPAC/2015/19579
Editor(s):
(1) Lichun Sun, Department of Medicine, Tulane University Health Sciences Center, USA.
Reviewers:
(1) Anonymous, Wrocław University of Technology, Poland.
(2) S. Srinivas Rao, Chemistry, JNT University Hyderabad, India.
Complete Peer review History: http://sciencedomain.org/review-history/10565

Short Communication

Received 17th June 2015
Accepted 23rd July 2015
Published 14th August 2015

ABSTRACT

Antibody-antigen interactions play a major role in many biological systems and can be used in sensors to capture target molecules. We investigated, as an example, the interaction behaviour of Picloram, a herbicide, which can contaminate fresh water supply, and its corresponding antibody. Antibody 3D homology modelling and antigen-antibody docking calculations followed by quantum mechanical calculations were used to understand antibody structures and binding mechanism, and to calculate antibody-antigen interaction energies. This study will guide experimental studies to develop antibody based filtration technique.

Keywords: Antibody; antigen; picloram; molecular modelling; antibody-antigen interactions.

**Corresponding author: E-mail: mohid@buet.ac.bd, theo.vandeven@mcgill.ca;*

1. INTRODUCTION

Antibodies have a wide range of applications. Antibody active paper filters and sensors can detect blood groups, viruses and the presence of herbicides and pesticides in water [1-4]. However, the antibody-antigen interactions on cellulosic materials are less understood [1,3]. Antibody contains two heavy chains and two light chains of amino acids [5,6]. Antibody has antigen binding fragments (Fab) that contain six specific zones, which are knowns as complementary determining regions (CDR): CDR L1-L3, and CDR H1-H3 [7]. These CDRs are antigen binding sites. Computational chemistry is used to understand antibody structure and antibody-antigen binding in-vivo and *In-vitro* [8-11]. X-ray crystallography and nuclear magnetic resonance are robust experimental techniques to determine Antibody structures, but are laborious, expensive and time consuming [12,13]. The 3D structure data of proteins, antibodies and nucleic acids are stored in Protein Data Bank (PDB) (www.pdb.org) [14], available as PDB file format. Currently about 110,000 PDB files are available with an approximate increasing rate of 9,500 per year [14], which is less than 0.001% of the billions of different antibodies human body can possibly generate [15]. Consequently, 3D homology modelling is the state of the art in structure-based protein engineering applications [9,13]. Homology based protein simulation programmes can predict 3D antibody structures [13]. These homology models search different identical fragments of the 3D antibody structures from the PDB database and join them to create the primary antibody structure. The primary model is optimized using different Molecular Mechanical Force Fields [12,13]; a few programmes provide the option to use quantum mechanics theories to optimize the very long chains of CDR H3 [8]. Possible antigen binding sites are identified from the optimized antibody structure, and antibody-antigen interactions are analyzed from antibody-antigen docking [8,9,13].

2. METHODS, RESULTS AND DISCUSSION

We calculated antibody-antigen interactions using molecular mechanics (MM) followed by quantum mechanics (QM). MM predicts large molecular structures, possible molecular interactions at a specific region, and initial starting point geometries for QM calculations. MM calculation requires a significant lower computation time. However, MM theories do not consider electrons in modelling calculation, which actually hold all molecules together. QM calculates the energy of state and electronic properties of the interacting molecules. The major limitation of QM methods is that they require longer computing time [16]. Molecular simulation combining MM and QM can be highly useful to accurately understand antibody structure and mechanism efficiently. This theoretical study will guide experimental studies to develop and regenerate an antibody based filtration technique [3,17-19], and to detoxify drugs and other toxic chemicals from the human body [20-22].

The antibody-antigen interactions at the molecular level are applied to Picloram (4-Amino-3,5,6-trichloropyridine-2-carboxylic Acid) and Picloram antibody. Picloram, a long lived herbicide can enters the fresh water supply and may cause health and environmental problems [23,24]. Antibody based electrochemical sensors and paper filters can detect and remove Picloram [18,19]. Hall et al identified the amino acid sequence of the anti-Picloram Fab [17,25,26] (Fig. A1; supplementary information). The Molecular Operating Environment 2011 (*MOE2011.10*) programme developed by Chemical Computing Group [27] was used to model the 3D structure of Picloram antibody, to identify possible binding sites, to analyze antibody-antigen interactions using antibody-antigen docking, and to predict the best antibody-antigen interaction. From *MOE2011.10* calculation the interacting antigen (Picloram) and antibody receptor atoms were extracted to run the semi-empirical quantum calculation PM6, which takes less computational time than *ab initio* [16]. GaussView 5.0.8 and Gaussian 09W programmes were used to run PM6 calculations. The interaction energies and electronic properties like delocalized molecular orbitals (DLMO) and electrostatic potentials (ESP) of PM6 calculated molecules were analyzed to identify the favourable and unfavourable interaction conditions.

The *MOE2011.10* 'Antibody Moduler' provides a flexible and automated graphical interface for antibody homology modelling. It employs a knowledge-based approach that features a built-in PDB database of the antibody structures, which allows for continuous updates [13,27]. The template search uses a sequence-to-profile alignment algorithm which ranks the templates by a structural score on the basis of the sequence similarity and identity. The structure scores range from 0 (not suitable for homology modelling purpose) to 100 (ideal protein

structure) [27]. To build up 3D anti-Picloram Fab, top scoring PDB templates for individual frames (FR) and CDR loops were chosen for light and heavy chains. The structure scores for top scoring variable heavy chain (*VH*) varied from 87.9% to 99.4%; and for the light chain (*LH*) templates the top score varied from 85.4% to 98.9% (Fig. A1b). Structure scores higher than 85% ensure the selection of antibody templates with physically realistic backbone structures. Once the top scoring homologous FR and CDR templates were found, the respective loop templates were joined accordingly, followed by optimization using Marck Molecular Force Field theory (MMFF94x) [13,27,28]. The energy of MMFF94x optimized structure was found -32.16 kcal/mol. The solvation effect on the optimized structure at Ph 7 was considered, and the ionization states and hydrogen positions in the optimized 3D structure were assigned using the Protonate 3D option [27]. After using this option, the energy of the modelled antibody at pH 7 was -242.78 kcal/mol. The MM calculation does not necessarily give accurate energies, however, the energy difference (-210.62 kcal/mol) qualifies more stable antibody structure considering the solvation effect.

The structural stability of the modelled Fab was also verified from the Phi(**φ**)- Psi(**ψ**) Plot, Ramachandran Plot [29] (Fig. 1a), which checks the stereochemical quality of a protein structure. The data points of the backbone torsion angles **φ** and **ψ** tend to cluster in favourable core regions (inside **green lines**) and allowed regions (inside **yellow lines**); the white areas are unfavourable regions because of steric hindrance. Fig. 1b shows the CDRs in the backbone structure of the modelled antibody Fab. The binding sites available in the 3D Fab structure were identified using *MOE2011.10,* which uses geometric methods to locate "Pockets" without the use of energy models [27]. Fig. 1c shows the van der Waals surfaces of the binding sites mapped with positive and negative regions, which are coloured in **red** and **blue**. The geometric positions and CDR receptor atoms of all possible binding sites were analyzed. Binding site 1, 2, 3, 7, 8 were adjacent to or surrounded by CDR receptor atoms. Other possible binding sites, such as 4, 5, 6, 9, 10, 11 were not related to CDR receptor atoms; therefore, these sites were excluded for further calculations.

After analyzing and sorting out the possible binding sites, the Picloram interactions were investigated at different binding sites using the Docking technique. Once the Picloram is placed inside the binding pocket, the *MOE2011.10* generates a number of possible orientations of Picloram, which were manually placed inside the pocket to allow them to interact with the receptor atoms. To calculate the optimal interactions from docking, the van der Waals interactions, electrostatic interactions, hydrophobic-hydrophilic interactions, hydrogen bonding, and interaction energies were considered. From the analysis of 120 Picloram-receptor atom interactions the best fit interaction was found, which was at binding site 7 surrounded by CDR H2 and L3 (Fig. 1d). The Picloram fits properly inside the van der Waals surface of the binding site (Fig. A2; supplementary information). Fig. 1e shows that the Picloram is positioned inside the binding pocket with compatible electrostatic interactions (i.e. Picloram's positive ends interact to receptor atoms' negative ends and vice versa), hydrophobic-hydrophobic interactions and polar-polar interactions. Fig. 1f shows the ligand interactions with different residues of the receptor atoms: Asparagine (Asn 61) and Lysine (Lys 63) of CDR H2, Tryptophan (Trp 115) of CDR L3 and Tryptophan (Trp 47) of *VH* FR.

After identifying the favourable Picloram-receptor atoms interaction, the receptor atoms and Picloram structures were extracted from *MOE2011.10* to run a semi-empirical PM6 calculation. PM6 calculated energies for receptor atoms, Picloram, and Picloram interacting with receptor atoms were -316.08, -113.47, and -482.00 kcal/mol, respectively. To understand the Picloram-receptor atom interaction, electronic properties such as DLMOs and ESPs were analyzed. Fig. 1g shows the electrostatic potential (ESP) surfaces of the Picloram-receptor atoms interactions. The Picloram molecule was found well surrounded by the receptor atoms and held by electrostatic interactions. ESP surfaces of the Picloram and receptor atoms before and after interactions are shown in Fig. A3 (see supplementary information). DLMOs of Picloram-receptor atoms interactions are shown in Figs. A4 and A5 (supplementary information). No strong electron overlap was found, either in the lowest unoccupied molecular orbital (LUMO) or the highest occupied molecular orbital (HOMO). However, a slight overlap of DLMO wave functions was found at different energy levels, such as: DLMO 360, which indicates the presence of a weak bond (Figs. A4-5; supplementary information).

The above analysis was conducted for pH 7. The PM6 calculation was also conducted on the

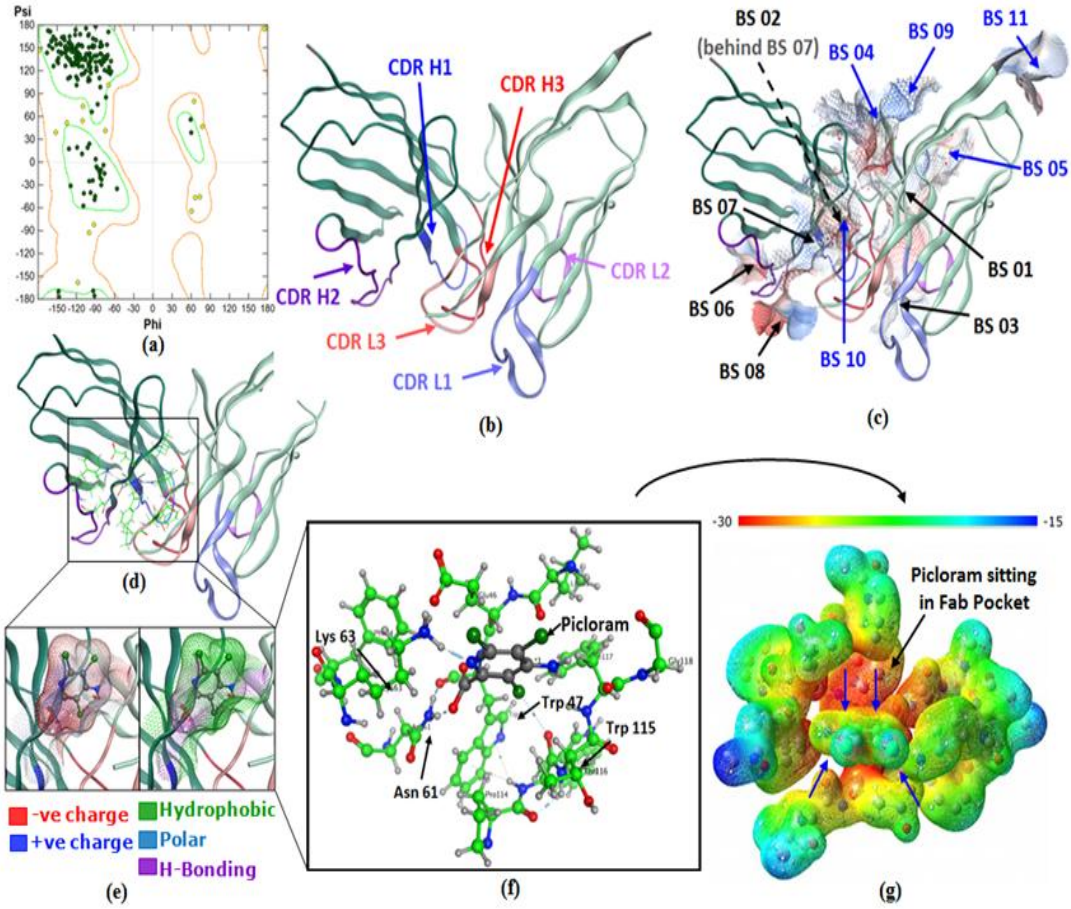

Fig. 1. (a) φ-ψ Plot of modelled anti-Picloram Fab: green points indicate core regions and yellow points indicate allowed regions; (b) CDRs positioned in Fab backbone. (c) Possible binding sites (BS) coloured in electrostatic surfaces: red colour is indicating negative regions and blue is positive. (d) Picloram interaction at binding site 7. (e) Picloram interaction in receptor atoms' pocket. (f) Picloram interaction with receptor atoms of CDR H2 (Asn 61, Lys 63), CDR L3 (Trp 115) and *VH* FR (Trp 47). (g) PM6 calculated electrostatic potential (ESP) surfaces of the Picloram-receptor atoms complex showing Picloram is held inside the pocket using electrostatic interactions; red colour is indicating negative regions and blue is positive

MOE2011.10 extracted molecules for alkaline (high pH) and acidic (low pH) conditions and the interaction energies were calculated (Table 1). The side chains of the residue molecules were protonated and deprotonated to match with changed pH. Table 1 shows that the Picloram and anti-Picloram Fab interaction is more stable at pH 7 ($E_{pH\ 7}$ = -52.45 kcal/mol) and highly unstable at acidic condition (E_{Acidic} = 206.99 kcal/mol). At acidic condition, the protonated molecules: Picloram and residue molecules of anti-Picloram Fab, cause highly unstable interaction.

Consequently, these calculations can be useful in developing antibody based filtration systems to filter Picloram and Picloram like chemicals. At neutral pH, the antibody based filter will capture Picloram. Once the filter is saturated, a back wash with acidic solution will release Picloram and regenerate the filtration system for reuse. These calculations confirm the experimental results from a separate study [3]. Besides the antibody based filtration technique, molecular studies of antibody-antigen interactions at different pH can be useful in detoxification of drug or toxic chemicals from the human body.

A separate compatibility test was performed to analyse the specificity of the modelled anti-Picloram Fab using Picloram and three other Picloram-like molecules: Fluroxypyr,

Table 1. Semi-empirical PM6 calculated picloram and anti-picloram fab interaction energy (kcal/mol) under different pH conditions

pH condition	Energies (kcal/mol)			
	Picloram, E_{ligand}	Receptor atoms, $E_{receptor\ atoms}$	Picloram interacting with receptor atoms, $E_{ligand+receptor\ atoms}$	Interaction energy, $E = E_{ligand+receptor\ atoms} - (E_{ligand} + E_{receptor\ atoms})$
Neutral	-113.47	-316.08	-482.00	-52.45
Alkaline	-113.47	-352.93	-457.13	9.27
Acidic	-64.68	93.43	235.74	206.99

Aminopyralid and Clopyralid, to validate the calculation methodology. The compatibility test predicted which of the Picloram-like molecule will interact with anti-Picloram Fab. The theoretical results were found to be consistent with the experimental results. The compatibility test results to validate the MOE calculation methodology are not shown in this study and will be discussed in a separate article.

3. CONCLUSION

Molecular modelling of Picloram and anti-Picloram Fab interactions at different pHs were calculated using 3D homology modelling, force field theory and quantum mechanical calculation. This method allowed understanding the structural and electronic properties of antibody-antigen interactions at possible binding sites, and calculating the antibody-antigen interaction energies at different pH conditions. The electronic properties and energies show that a strong interaction of Picloram and anti-Picloram Fab occurs at pH 7 but not when acidic. This information may be useful in developing and regenerating antibody based sensors and filtration systems.

ACKNOWLEDGEMENT

This research was supported by SENTINEL Bioactive Paper Network funded by the NSERC-CRSNG, and an NSERC Discovery Grant. Authors acknowledge SENTINEL Bioactive Paper Network for funding, and Drs. Chris Hall and Chris Williams for useful discussion.

COMPETING INTERESTS

Authors have declared that no competing interests exist.

REFERENCES

1. Khan MS, Thouas G, Shen W, Whyte G, Garnier G. Paper diagnostic for instantaneous blood typing. Analytical Chemistry. 2010;82:4158-4164.
2. Pelton R. Bioactive paper provides a low-cost platform for diagnostics. Trends in Analytical Chemistry. 2009;28:925-942.
3. Venkataprasad C. Adsorption of herbicides and bacteria using pulp fibers. Mechanical and Industrial Engineering, Master of Applied Science Thesis, Concordia University, Montreal, Canada. 2009;1-58.
4. Khan MS, Pande T, van de Ven TGM. Qualitative and quantitative detection of T7 bacteriophages using paper based sandwich ELISA. Colloids and Surfaces B: Biointerfaces. 2015;132:264-270.
5. Mikkelsen SR, Corton E. Bioanalytical Chemistry. John Wiley & Sons, Inc., Publication, New Jersey; 2004.
6. Young CR. Structural requirements for immunogenicity and antigenicity, in: Atassi MZ, Oss CJV, Absolom DR. (Eds.), Molecular Immunology, Marcel Dekker, Inc., New York. 1984;1-14.
7. Elgert KD. Immunology: Understanding the immune system, 2nd ed., Wiley-Blackwell; 2009.
8. Kuroda D, Shirai H, Jacobson MP, Nakamura H. Computer-aided antibody design. Protein Engineering, Design & Selection. 2012;25:1-15.
9. Sivasubramanian A, Sircar A, Chaudhury S, Gray JJ. Toward high-resolution homology modeling of antibody fv regions and application to antibody-antigen docking. Proteins: Structure, Function, and Bioinformatics. 2009;74:497–514.
10. Das Thakur M, Salangsang F, Landman AS, Sellers WR, Pryer NK, Levesque MP, Dummer R, McMahon M, Stuart DD. Modelling vemurafenib resistance in melanoma reveals a strategy to forestall drug resistance. Nature. 2013;494:251-255.
11. Skakauskas V, Katauskis P, Skvortsov A, Gray P. Modelling effects of internalized antibody: A simple comparative study. Theoretical Biology and Medical Modelling. 2014;11:11.

12. Sircar A, Kim ET, Gray JJ. Rosetta antibody: Antibody variable region homology modeling server. Nucleic Acids Research. 2009;37:W474-W479.
13. Almagro JC, Beavers MP, Hernandez-Guzman F, Maier J, Shaulsky J, Butenhof K, Labute P, Thorsteinson N, Kelly K, Teplyakov A, Luo J, Sweet R, Gilliland GL. Antibody modeling assessment. Proteins: Structure, Function and Bioinformatics. 2011;79:3050-3066.
14. RCSB PDB protein data bank: An information portal to biological macromolecular structures, rutgers. The State University of New Jersey and University of California, San Diego (UCSD); 2015.
15. Fanning LJ, Connor AM, Wu GE. Short analytical review: Development of the immunoglobulin repertoire. Clinical Immunology and Immunopathology. 1996; 79:1-14.
16. Lewars EG. Computational chemistry: Introduction to the theory and applications of molecular and quantum mechanics. 2 ed., Springer, New York; 2011.
17. Deschamps RJA, Hall JC, McDermottg MR. Polyclonal and monoclonal enzyme immunoassays for picloram detection in water, soil, plants and urine. Journal of Agriculture and Food Chemistry. 1990;38: 1881-1886.
18. Chen L, Zeng G, Zhang Y, Tang L, Huang D, Liu C, Pang Y, Luo J. Trace detection of picloram using an electrochemical immunosensor based on three-dimensional gold nanoclusters. Analytical Biochemistry. 2010;407:172-179.
19. Tang L, Zeng GM, Shen GL, Li YP, Zhang Y, Huang DL. Rapid detection of picloram in agricultural field samples using a disposable immunomembrane-based electrochemical sensor. Environmental Science & Technology. 2008;42:1207-1212.
20. Strazielle N, Khuth ST, Ghersi-Egea JFO. Detoxification systems, passive and specific transport for drugs at the blood-CSF barrier in normal and pathological situations. Advanced Drug Delivery Reviews. 2004;56:1717-1740.
21. Benet LZ, Spahn-Langguth H, Iwakawa S, Volland C, Mizuma T, Mayer S, Mutschler E, Lin ET. Predictability of the covalent binding of acidic drugs in man. Life Sciences. 1993;53:PL141-PL146.
22. Zhang K, Mack P, Wong KP. Glutathione-related mechanisms in cellular resistance to anticancer drugs. International Journal of Oncology. 1998;12:871-882.
23. Hall JC, Deschamps RJ, Krieg KK. Immunoassays for the detection of 2, 4-D and picloram in river water and urine. Journal of Agricultural and Food Chemistry. 1989;37:981-984.
24. Horsman J, McLean MD, Olea-Popelka FC, Hall JC. Picloram resistance in transgenic tobacco expressing an anti-picloram scFv antibody is due to reduced translocation. Journal of Agriculture and Food Chemistry. 2007;55:106-112.
25. Yau KYF, Tout NL, Trevors JT, Lee H, Hall JC. Bacterial expression and characterization of a picloram-specific recombinant fab for residue analysis. Journal of Agriculture and Food Chemistry. 1998;46:4457-4463.
26. Olea-Popelka F, McLean MD, Horsman J, Almquist K, Brandle JE, Hall JC. Increasing expression of an anti-picloram single-chain variable fragment (ScFv) antibody and resistance to picloram in transgenic tobacco (*Nicotiana tabacum*). Journal of Agriculture and Food Chemistry. 2005;53:6683-6690.
27. Molecular Operating Environment (MOE), 2011.10, Chemical Computing Group Inc., Montreal, QC, Canada, H3A 2R7; 2011.
28. Halgren TA. Merck molecular force field. I. Basis, Form, Scope, Parameterization, and Performance of MMFF94*. Journal of Computational Chemistry. 1996;17:490-519.
29. Ramachandran GN, Ramakrishnan C, Sasisekharan V. Stereochemistry of polypeptide chain configurations. Journal of Molecular Biology. 1963;7:95-99.

Peer-review history:
The peer review history for this paper can be accessed here:
http://sciencedomain.org/review-history/10565